

Drift Removal for Time Series Data Using Quantile Trend Filtering

Halley Brantley* Joseph Guinness[†] and Eric C. Chi[‡]

Abstract

The text of your abstract. 200 or fewer words.

Keywords: 3 to 6 keywords, that do not appear in the title

*Department of Statistics, North Carolina State University, Raleigh, NC 27695 (E-mail: hlbrantl@ncsu.edu)

[†]Department of Biological Statistics and Computational Biology, Cornell University, Ithaca, NY 14853 (E-mail: guinness@cornell.edu)

[‡]Department of Statistics, North Carolina State University, Raleigh, NC 27695 (E-mail: eric_chi@ncsu.edu).

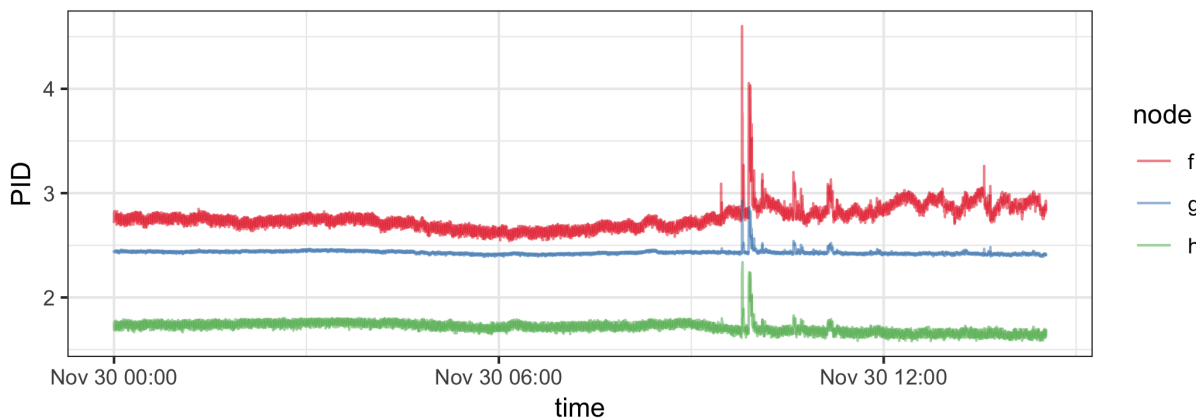
1 Introduction

The use of low-cost, portable, air quality sensors has increased dramatically in the last decade. These sensors can provide an un-calibrated measure of a variety of pollutants in near real time, but deriving meaningful information from sensor data remains a challenge (Snyder et al., 2013). The “SPod” is a low-cost sensor currently being investigated by researchers at the U.S. Environmental Protection Agency to detect volatile organic compound (VOC) emissions from industrial facilities (Thoma et al., 2016). To reduce cost and power consumption of the SPod, the temperature and relative humidity of the air presented to the photoionization detectors (PIDs) is not controlled and as a result the output signal exhibits a slowly varying baseline drift on the order of minutes to hours (Fig. 1).

There have been a number of other occasions when researchers have sought to estimate the trend in the quantiles of a random variable over time or another co-variate given noisy observations of that variable. Nychka et al. (1995) estimated smooth quantile curves of friction profiles of syringes in order to automate their quality assessment procedures. Ning et al. (2014) proposed a method for separating chromatogram peaks from the smooth baseline and noise present in the measurements. Brantley et al. (2014) examined air pollutant measurements collected using a monitoring vehicle and proposed using a smooth baseline trend as an estimate of regional background pollution.

A variety of approaches have been proposed for estimating quantile trends. Koenker

Figure 1: Example of 3 co-located SPod PID sensor readings.



and Bassett (1978) was the first to propose the use of the check loss function to estimate conditional quantiles. Given a design matrix $\mathbf{X} \in \mathbb{R}^{n \times p}$ and continuous responses $y \in \mathbb{R}^n$, we estimate a regression vector $\theta \in \mathbb{R}^p$ so that $\mathbf{X}\theta$ is a good approximation of the τ th quantile of y conditional on x . The regression vector θ is estimated by finding the minimizer of $\rho_\tau(y - X\theta)$ where $\rho_\tau(z) = \sum_{i=1}^n z_i(1 - \mathbf{I}(z_i < 0))$ is the check-loss function and \mathbf{I} is the indicator function.

In the trend filtering problem (Kim et al., 2009; Tibshirani, 2014), one is interested in finding an adaptive polynomial approximation to noisy data $y \in \mathbb{R}^n$ by solving the following convex problem.

$$\arg \min_{\theta} \frac{1}{2n} \|y - \theta\|_2^2 + \lambda \|\mathbf{D}^{(k+1)}\theta\|_1, \quad (1)$$

where $\lambda \geq 0$ is a regularization parameter that trades off the emphasis on the data fidelity term and the matrix $\mathbf{D}^{(k+1)} \in \mathbb{R}^{(n-k-1) \times n}$ is the discrete difference operator of order $k+1$. To understand the purpose of penalizing $\mathbf{D}^{(k+1)}$ consider the difference operator when $k=0$.

$$\mathbf{D}^{(1)} = \begin{pmatrix} -1 & 1 & 0 & \cdots & 0 & 0 \\ 0 & -1 & 1 & \cdots & 0 & 0 \\ \vdots & & & & & \\ 0 & 0 & 0 & \cdots & -1 & 1 \end{pmatrix} \quad (2)$$

Thus, $\|\mathbf{D}^{(1)}\theta\|_1 = \sum_{i=1}^{n-1} |\theta_i - \theta_{i+1}|$ which is just total variation denoising in one dimension. The penalty incentivizes solutions which are piece-wise constant. For $k \geq 1$, the difference operator $\mathbf{D}^{(k+1)} \in \mathbb{R}^{(n-k-1) \times n}$ is defined recursively as follows

$$\mathbf{D}^{(k+1)} = \mathbf{D}^{(1)}\mathbf{D}^{(k)}. \quad (3)$$

By penalizing the $k+1$ fold composition of the discrete difference operator, we obtain solutions which are piecewise polynomials of order k .

We propose to use the trend filtering penalty with the check loss function to produce a non-parametric quantile regression estimate for removing trends in time series. The formulation was proposed by Kim et al. (2009) as a possible extension of ℓ_1 -trend filtering but not studied. Moreover we extend the basic framework to ensure non-crossing while

modeling multiple quantiles. We also implement a parallel ADMM algorithm for series that are too large to be computed simultaneously and proposed a modified criteria for choosing the smoothing parameter. We demonstrate through simulation studies that our proposed model provides better or comparable estimates of non-parametric quantile trends than existing methods and is a more effective method of drift removal for low-cost air quality sensors.

2 Methods

2.1 Quantile Trend Filtering

We combine the ideas of quantile regression and trend filtering, namely consider the case where the design \mathbf{X} is the identity matrix. For a single quantile level τ the estimation of the quantile trend filtering model can be posed as the following optimization problem.

$$\min_{\theta} \rho_{\tau}(y - \theta) + \lambda \|\mathbf{D}^{(k)}\theta\|_1, \quad (4)$$

where λ is a non-negative tuning parameter. As with the classic quantile regression, the quantile trend filtering problem is a linear program which can be solved by a number of free or commercial solvers. In many cases, including ours, we are interested in estimating multiple quantiles simultaneously. We also want to ensure that our quantile estimates are valid by enforcing the constraint that if $\tau_2 > \tau_1$ then $Q(\tau_2) \geq Q(\tau_1)$. Given quantiles $\{\tau_1, \dots, \tau_J\}$ such that $\tau_1 < \tau_2 < \dots < \tau_J$, the optimization problem becomes

$$\min_{\theta} \sum_{j=1}^J \left[\frac{1}{n} \rho_{\tau_j}(y - \theta_j) + \lambda_j \|\mathbf{D}^{(k)}\theta_j\|_1 \right] \quad (5)$$

$$\text{subject to: } \theta_{1i} \leq \theta_{2i} \leq \dots \leq \theta_{Ji} \text{ for all } i, \quad (6)$$

where $\theta = (\theta_1, \dots, \theta_J)$ and $\theta_j \in \mathcal{R}^n$. The additional constraints are linear in the parameters so the non-crossing quantile trends can still be estimated by a number of available solvers.

The number of parameters to be estimates is equal to the number of observations multiplied by the number of quantiles of interest. As the size of the data and the number of quantiles grows, all solvers will eventually break.

2.2 ADMM for Big Data

To our knowledge, no one has addressed the problem of finding smooth quantile trends of series that are too large to be processed simultaneously. We propose an alternating direction method of multipliers (ADMM) algorithm for solving large problems in a piecewise fashion. The ADMM algorithm is fully described by Boyd et al. (2011); Gabay and Mercier (1975); Glowinski and Marroco (1975). We apply the consensus ADMM algorithm to the the quantile regression trend filtering problem given in Eq. 5, by dividing our observed series y into overlapping windows $\{y_1, \dots, y_M\}$, we then estimate the trend separately in each window while constraining the overlapping pieces of the trends to be equal.

Algorithm 1 ADMM algorithm for quantile trend filtering with windows

Given y divided into overlapping windows $\{y_1, \dots, y_M\}$ and quantiles $\{\tau_1 < \dots < \tau_J\}$

initialize:

$$\theta_{j,m}^{(0)} = \arg \min \sum_{j=1}^J \rho_{\tau_j}(y_m - \theta_{j,m}) + \lambda \|D\theta_{j,m}\|_1 \text{ subject to } \theta_{1,m} < \dots < \theta_{J,m}.$$

$\bar{\theta}_{j,m}^{(0)}$ is the mean of $\theta_{j,m}^{(0)}$ and all overlapping windows.

$$\omega_{j,m}^{(0)} = \gamma(\theta_{j,m}^{(0)} - \bar{\theta}_{j,m}^{(0)})$$

repeat

$$\theta_{j,m}^{(q)} = \arg \min \sum_{j=1}^J \rho_{\tau_j}(y_m - \theta_{j,m}) + \lambda \|D\theta_{j,m}\|_1 + \omega_{j,m}^{(q-1)T}(\theta_{j,m} - \bar{\theta}_{j,m}^{(q-1)}) + \frac{\gamma}{2} \|\theta_{j,m} - \bar{\theta}_{j,m}^{(q-1)}\|_2^2$$

subject to $\theta_{1,m} < \dots < \theta_{J,m}$

$\bar{\theta}_{j,m}^{(q)}$ is the mean of $\theta_{j,m}^{(q)}$ and all overlapping windows.

$$\omega_{j,m}^{(q)} = \omega_{j,m}^{(q-1)} + \gamma(\theta_{j,m}^{(q)} - \bar{\theta}_{j,m}^{(q)})$$

until convergence

return Non-overlapping sequence of $\bar{\theta}_{j,m}^{(q)}$ for all j, m .

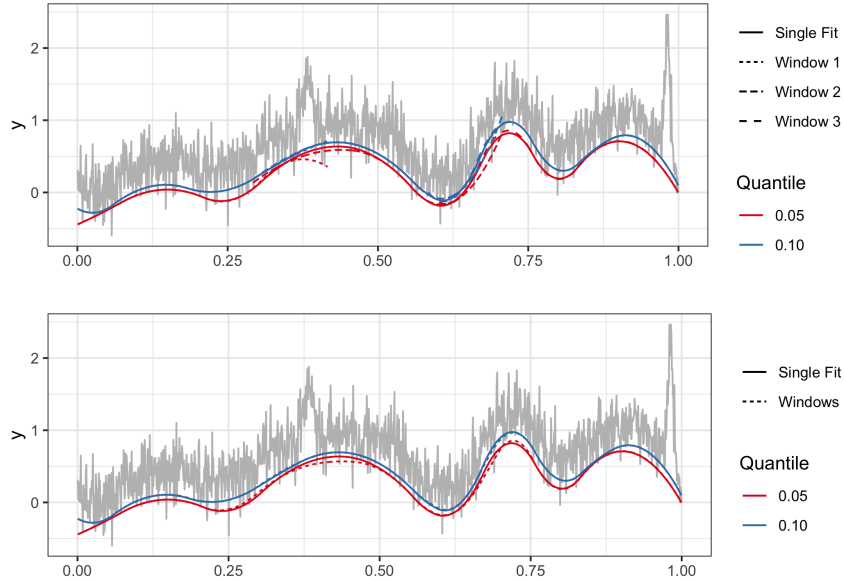
We used the stopping criteria described by Boyd et al. (2011). The criteria are based

on the primal and dual residuals which represent the residuals for the primal and dual feasibility, respectively. The primal and dual residuals are defined as

$$r_p^{(q)} = \sqrt{\sum_{m=1}^M \left(\theta_{j,m}^{(q)} - \bar{\theta}_{j,m}^{(q)} \right)^2} \quad (7)$$

$$r_d^{(q)} = \gamma \sqrt{\sum_{m=1}^M \left(\bar{\theta}_{j,m}^{(q)} - \bar{\theta}_{j,m}^{(q-1)} \right)^2} \quad (8)$$

Figure 2: (Top) Windows fit separately compared to simultaneous fit, no signal present. (Bottom) Windows fit with our ADMM algorithm which converged in 7 iterations.



Given N equal to the total number of elements in $\bar{\theta}$ and values for ϵ_{abs} and ϵ_{rel} , the algorithm is stopped when

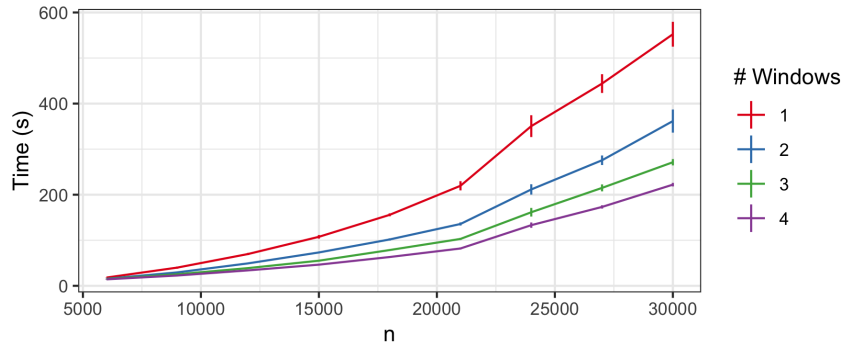
$$r_p^{(q)} < \epsilon_{abs} \sqrt{N} + \epsilon_{rel} \max(\|\theta_{j,m}^{(q)}\|_2, \|\bar{\theta}_{j,m}^{(q)}\|_2) \quad (9)$$

$$r_d^{(q)} < \epsilon_{abs} \sqrt{N} + \epsilon_{rel} \sqrt{\sum_{m=1}^M \left(\omega_{j,m}^{(q)} \right)^2} \quad (10)$$

Timing experiments illustrate the advantages of using our ADMM algorithm even on datasets where solving the problem simultaneously is possible. We use from one to four

windows for each data size with an overlap of 500. The windows algorithm was run until the stopping criteria were met using $\epsilon_{abs} = 0.01$ and $\epsilon_{rel} = 0.001$. For each data size, n , 25 datasets were simulated using the peaks simulation design described below and trends for three quantiles were fit simultaneously: 0.05, 0.1, and 0.15 using a $\lambda = n/5$.

Figure 3: Timing experiments comparing quantile trend filtering with varying numbers of windows by data size.



2.3 Smoothing parameter choice

Our method can easily handle missing data by changing the check loss function to output 0 for missing values. This allows us to leave out validation observations that can be used to select the tuning parameter λ and to compare method performance on real data. A number of methods have been proposed for selecting the quantile regression smoothing spline tuning parameter Yuan (2006). Koenker et al. (1994) relate λ to the number of interpolated points $p_\lambda = \sum I(y_i = \hat{g}_i(x_i))$, which can be thought of as active knots, they propose the Schwarz criterion for the selection of λ

$$\text{SIC}(p_\lambda) = \log[n^{-1} \sum \rho_\tau(y_i - \hat{g}(x_i))] + \frac{1}{2n} p_\lambda \log n \quad (11)$$

The traditional Bayesian Information Criterion (BIC) is given by

$$\text{BIC}(s) = -2 \log(L\{\hat{\theta}(s)\}) + \nu(s) \log n \quad (12)$$

where $\theta(s)$ is the parameter θ with those components outside s being set to 0, and $\nu(s)$ is the number of components in s . If we assume an asymmetric Laplace likelihood $L(y|\theta) =$

$\left(\frac{\tau^n(1-\tau)}{\sigma}\right)^n \exp\left\{-\sum_i \rho_\tau\left(\frac{y_i-\theta_i}{\sigma}\right)\right\}$ and the number of non-zero elements of $D\theta$ as df

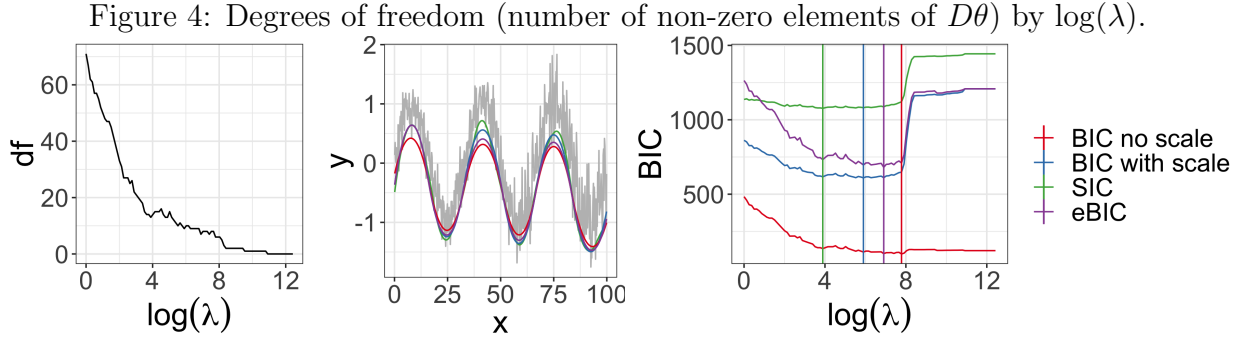
$$\text{BIC}(df) = 2 \sum_i \frac{1}{\sigma} \rho_\tau(y_i - \theta_i) + df \log n \quad (13)$$

We can choose any $\sigma > 0$ and have found empirically that $\sigma = \frac{1-|1-2\tau|}{2}$ produces stable estimates. Chen and Chen (2008) proposed the extended BIC for large parameter spaces

$$\text{BIC}_\gamma(s) = -2 \log(L\{\hat{\theta}(s)\}) + \nu(s) \log n + 2\gamma \log \binom{P}{j}, \quad \gamma \in [0, 1] \quad (14)$$

where P is the total number of possible parameters and j is the number of parameters included in given model. We used this criteria with $\gamma = 1$, $P = n - k$ where k is the order of the differencing matrix and $j = \nu(s)$ is the number of non-zero entries in $D^{(k)}\theta$.

We used a single dataset to illustrate the difference between the scaled, unscaled and extended BIC criteria.

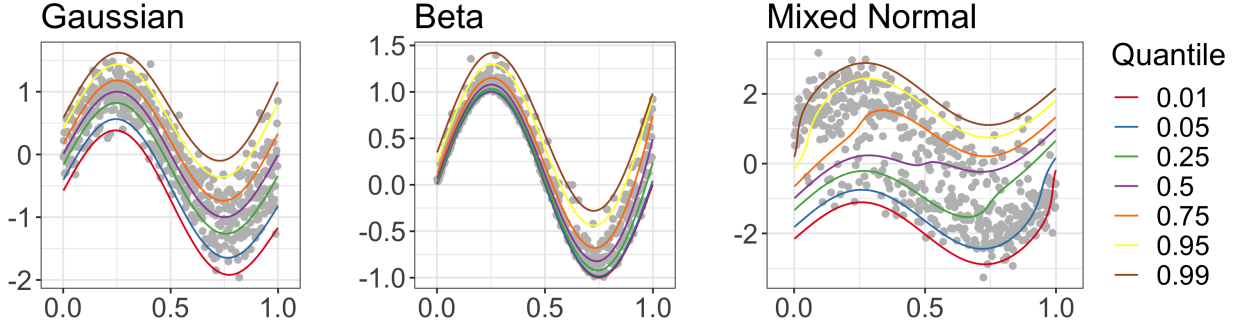


3 Simulation Studies

3.1 Estimating Quantiles

We compare the performance of our quantile trend filtering method with the three previously published methods using designs proposed by Racine and Li (2017). The methods compared are: `npqw` which is the quantile-ll method described in Racine and Li (2017), code was obtained from the author; `qsreg` in the `fields` R package and described in Oh et al. (2011); `rqss` available in the `quantreg` package and described in Koenker et al. (1994). The

Figure 5: Simulated data with true quantiles $\tau \in \{0.01, 0.05, 0.25, 0.5, .75, 0.95, 0.99\}$



smoothing parameter λ for the **rqss** method is chosen using a grid search and minimizing the SIC criteria as described in Koenker et al. (1994). We further compare three criteria for choosing the smoothing parameter for our detrend method: **detrendr_SIC**: Our method where we minimize $\sum_i \rho_\tau(y_i - \theta_i) + \lambda \|D\theta\|_1$ and λ is chosen using SIC (Koenker et al., 1994). **detrendr_valid**: Our method where lambda is chosen by leaving out every 5th observation as a validation data set and minimizing the evaluating the check loss function evaluated at the validation data. **detrendr_eBIC**: the new criteria we have proposed based on the extended BIC proposed by Chen and Chen (2008).

Three simulation designs from Racine and Li (2017) were considered. For all designs X_i was generated as a uniformly spaced sequence in $[0, 1]$ and the response Y was generated as

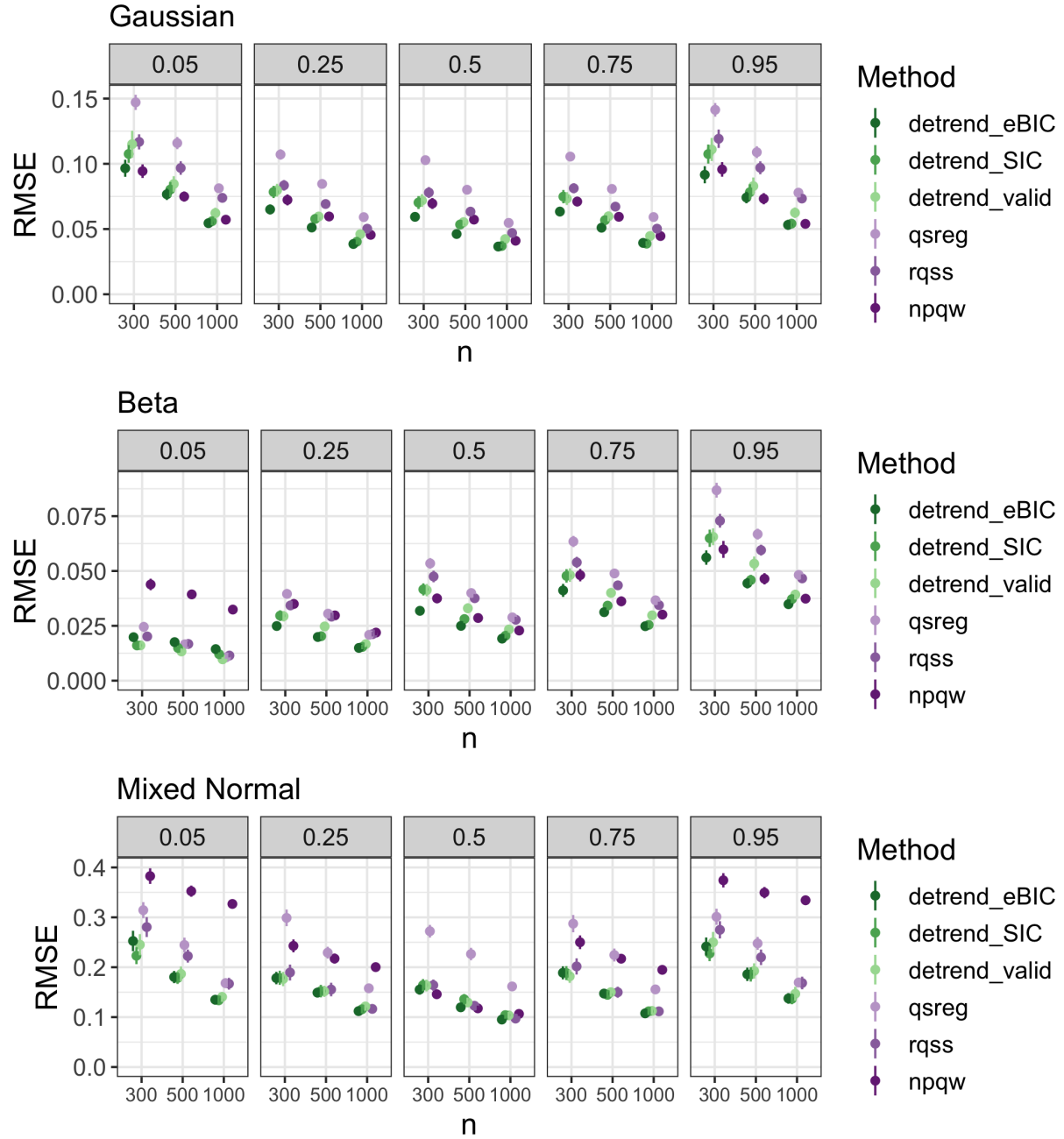
$$Y_i = \sin(2\pi x_i) + \epsilon_i(x_i)$$

The three error distributions considered were

- Gaussian: $\epsilon_i(x_i) \sim N\left(0, \left(\frac{1+x_i^2}{4}\right)^2\right)$
- Beta: $\epsilon_i \sim \text{Beta}(1, 11 - 10x_i)$
- Mixed normal: ϵ_i is simulated from a mixture of $N(-1, 1)$ and $N(1, 1)$ with mixing probability x_i .

100 datasets were generated of sizes 300, 500 and 1000. The MSE was calculated as $\frac{1}{n} \sum_i (\hat{q}_\tau(x_i) - q_\tau(x_i))^2$. The plots below show the mean MSE \pm twice the standard error by method, quantile level and sample size.

Figure 6: RMSE by design, method, quantile and data size.



In all of the designs the proposed detrend methods are either better than or comparable to existing methods. The npqw method performs particularly poorly in the mixed normal design, due to the fact that it assumes the data comes from a scale-location model which is violated in this case.

3.2 Peak Detection

We use another simulation design based on the applied problem we aim to solve. We assume that the measured data can be represented by

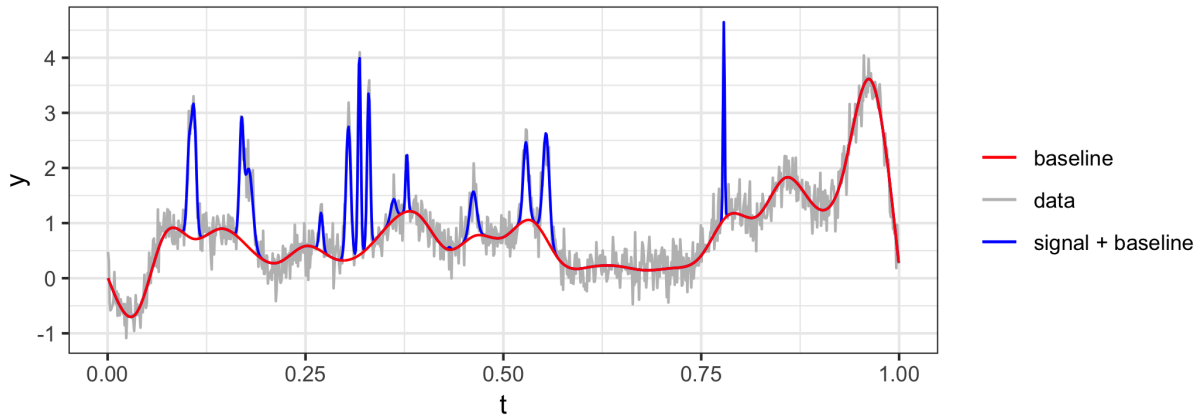
$$Y(t) = s(t) + b(t) + \epsilon(t) \quad (15)$$

where $s(t)$ is the true signal at time t , $b(t)$ is the drift component that varies smoothly over time and $\epsilon(t) \sim N(0, \sigma^2)$ is an error component. We assume t is a uniformly spaced sequence of time points between 0 and 1. We generate $b(t)$ using a cubic natural spline basis function with degrees of freedom sampled from $n/50$ to $n/25$ with equal probability, and coefficients drawn from an exponential distribution with rate 1. The true signal function is assumed to be zero with Gaussian peaks. The number of peaks is sampled from $n/100$ to $n/50$ with equal probability with centers uniformly distributed between 0.1 and 0.9 and bandwidths uniformly distributed between $1/n$ and $5/n$ and areas uniformly distributed between 0 and $20/n$. One hundred datasets were generated for $n = \{300, 500, 1000, 5000\}$. We compare the methods ability to estimate the true quantiles of $b(t) + \epsilon$ for $\tau \in \{0.01, 0.05, 0.1\}$ and calculate the root mean squared error (RMSE).

In addition to the RMSE we also calculated the signal miss-classification rate. We first classified the “true” peaks function into signal or not based on a threshold of 0.1. We then classified the detrended data using three different thresholds and calculated the fraction miss-classified. An illustration of the observations classified as signal after detrending compared to the “true signal” is shown in Fig. 9.

Our detrend_BIC method performs the best overall in terms of both RMSE and miss-classification rate. The lowest miss-classification rates were obtained using the detrend_eBIC method and a threshold of 1 for all data sizes. While qsreg was competitive with our method

Figure 7: Example of simulated peaks, baseline, and observed measurements.



in some cases, both the RMSE and miss-classification rate increased substantially with the size of the dataset.

Figure 8: Example signal classification using threshold. Red indicates true signal > 0.1 , blue indicates classified as signal after baseline removal using eBIC detrendr and a threshold of 1.

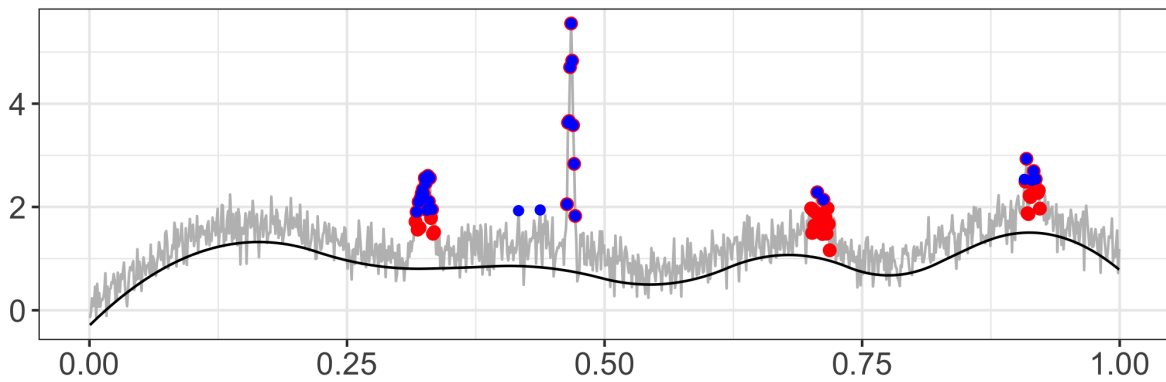
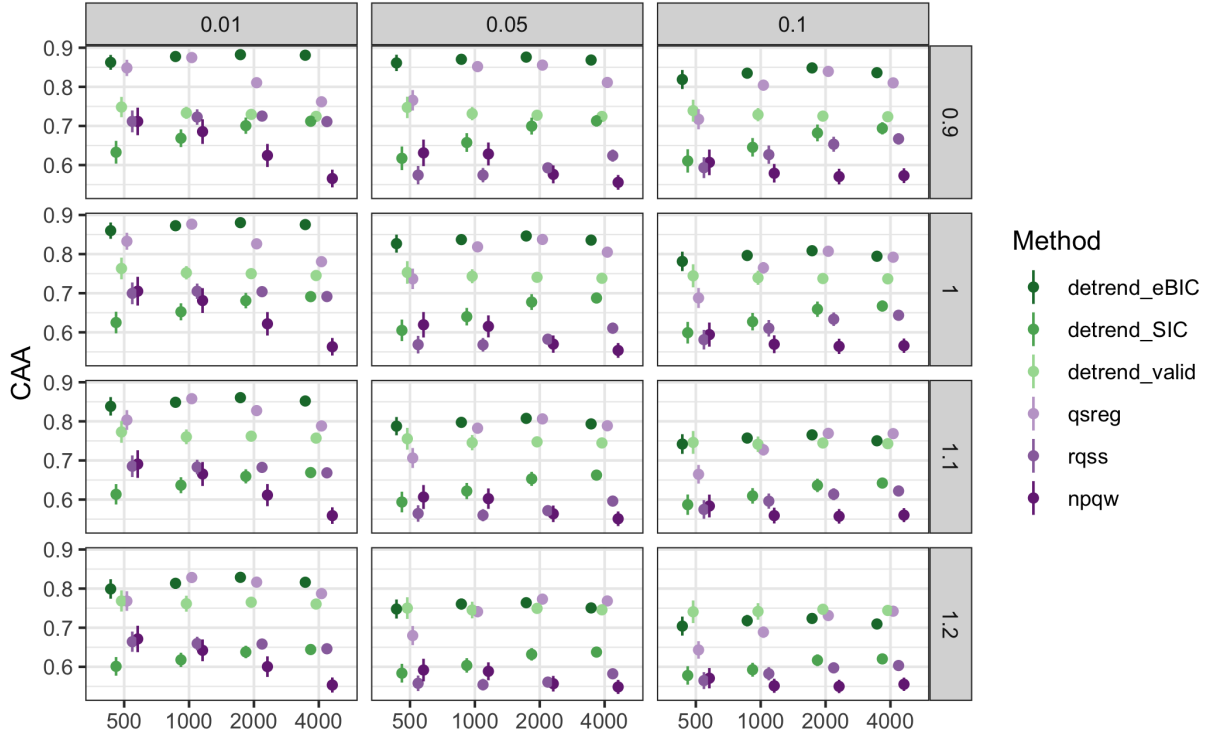


Figure 9: Class averaged accuracy by threshold, data size, and method (1 is best 0.5 is worst).



4 Application

We compared our detrend method with the eBIC criteria with the qsreg method on a subset of the real data since the qsreg method cannot handle all 15 hours simultaneously. We estimate the baseline trend using both the 5th and 10th quantiles and then classify the signal as any observation above the median plus 2.5 times the median absolute deviation after the baseline trend removal. We report both the confusion matrices and the normalized mutual information (NMI) score.

Our windowed detrend method was used to removed the baseline drift from low cost air quality sensors so that the signal could be categorized using a simple threshold. The measurements were first standardized to have mean zero and variance 1. Three quantile levels for estimating the baseline trend were compared. The total dataset consisted of 52,322 observations per node. The signal thresholds were set using the first 15,000 observations

Figure 10: Variation of Information between sensor nodes after trend removal by quantile and method and thresholding by factor of MAD.

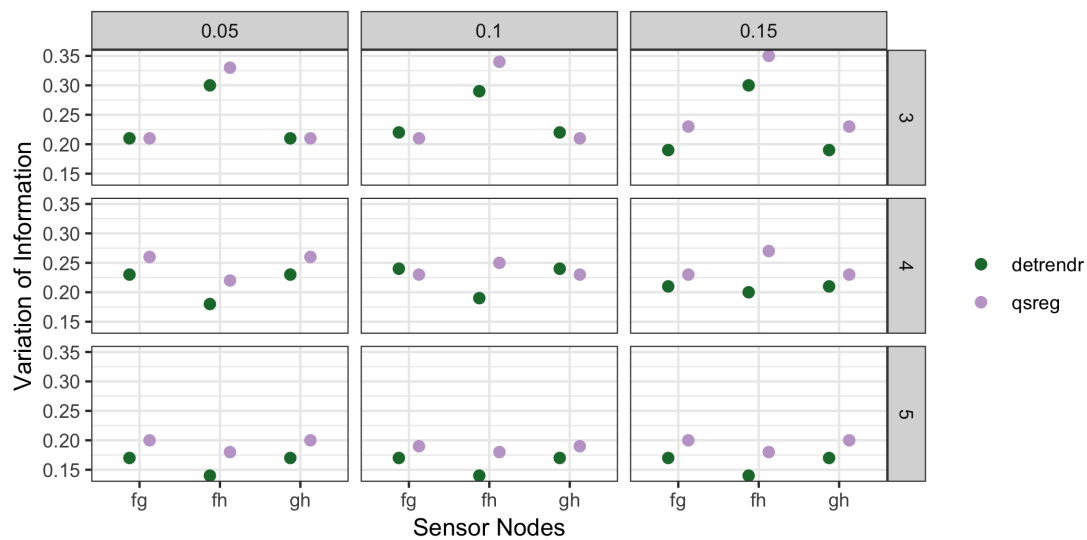


Figure 11: Rugplot showing locations of signal after baseline removal using detrendr estimate of 10th quantile.

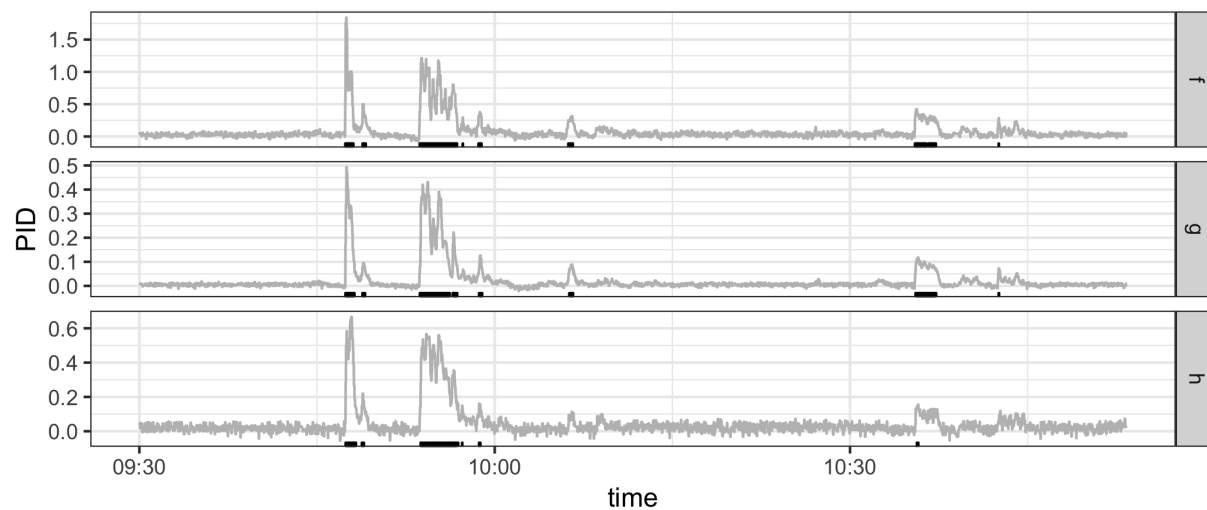


Figure 12: Low cost sensor data after drift removal using windowed detrend with eBIC.

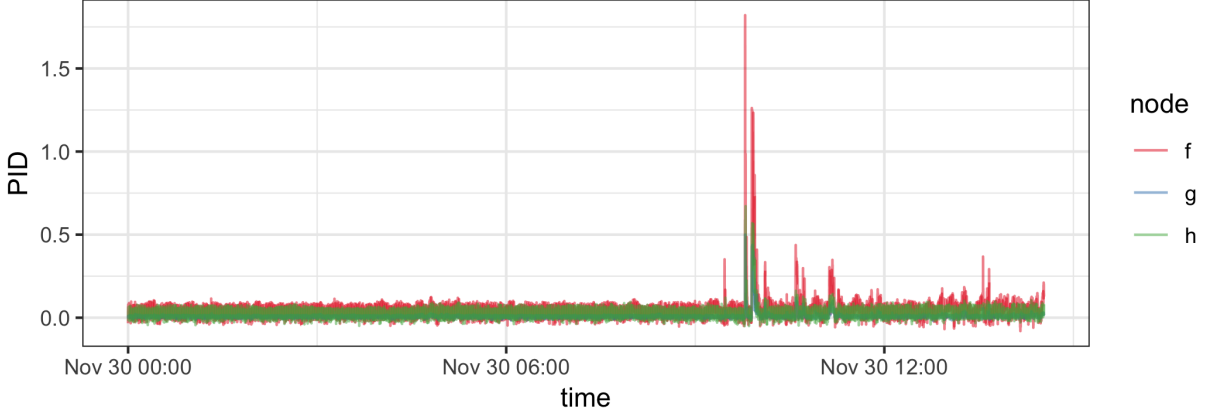


Table 1: Confusion matrices for 3 SPod nodes after baseline removal.

	h = 0		h = 1	
	g = 0	g = 1	g = 0	g = 1
f = 0	51123	386	3	29
f = 1	108	318	16	337

where it was known no signal was present. The thresholds were set as 3 times the standard deviation plus the mean of observations in this time period. The total number of seconds of signal for each node as well as the number of seconds where multiple nodes both reported signal is shown in Table 1. Table 2 shows the fraction of observations with different signal classifications by node combination.

5 Conclusion

SUPPLEMENTARY MATERIAL

R-package for detrend routine: R-package `detrendr` containing code to perform the diagnostic methods described in the article. The package also contains all datasets used as examples in the article. (GNU zipped tar file)

6 References

References

- Boyd, S., Parikh, N., Chu, E., Peleato, B., Eckstein, J., et al. (2011), “Distributed optimization and statistical learning via the alternating direction method of multipliers,” *Foundations and Trends® in Machine learning*, 3, 1–122.
- Brantley, H., Hagler, G., Kimbrough, E., Williams, R., Mukerjee, S., and Neas, L. (2014), “Mobile air monitoring data-processing strategies and effects on spatial air pollution trends,” *Atmospheric measurement techniques*, 7, 2169–2183.
- Chen, J. and Chen, Z. (2008), “Extended Bayesian information criteria for model selection with large model spaces,” *Biometrika*, 95, 759–771.
- Gabay, D. and Mercier, B. (1975), *A dual algorithm for the solution of non linear variational problems via finite element approximation*, Institut de recherche d’informatique et d’automatique.
- Glowinski, R. and Marroco, A. (1975), “Sur l’approximation, par éléments finis d’ordre un, et la résolution, par pénalisation-dualité d’une classe de problèmes de Dirichlet non linéaires,” *Revue française d’automatique, informatique, recherche opérationnelle. Analyse numérique*, 9, 41–76.
- Kim, S.-J., Koh, K., Boyd, S., and Gorinevsky, D. (2009), “ ℓ_1 Trend Filtering,” *SIAM Review*, 51, 339–360.
- Koenker, R. and Bassett, G. (1978), “Regression Quantiles,” *Econometrica*, 46, 33–50.
- Koenker, R., Ng, P., and Portnoy, S. (1994), “Quantile smoothing splines,” *Biometrika*, 81, 673–680.
- Ning, X., Selesnick, I. W., and Duval, L. (2014), “Chromatogram baseline estimation and denoising using sparsity (BEADS),” *Chemometrics and Intelligent Laboratory Systems*, 139, 156 – 167.

- Nychka, D., Gray, G., Haaland, P., Martin, D., and O’connell, M. (1995), “A nonparametric regression approach to syringe grading for quality improvement,” *Journal of the American Statistical Association*, 90, 1171–1178.
- Oh, H.-S., Lee, T. C. M., and Nychka, D. W. (2011), “Fast Nonparametric Quantile Regression With Arbitrary Smoothing Methods,” *Journal of Computational and Graphical Statistics*, 20, 510–526.
- Racine, J. S. and Li, K. (2017), “Nonparametric conditional quantile estimation: A locally weighted quantile kernel approach,” *Journal of Econometrics*, 201, 72–94.
- Snyder, E., Watkins, T., Solomon, P., Thoma, E., Williams, R., Hagler, G., Shelow, D., Hindin, D., Kilaru, V., and Preuss, P. (2013), “The changing paradigm of air pollution monitoring.” *Environmental science & technology*, 47, 11369.
- Thoma, E. D., Brantley, H. L., Oliver, K. D., Whitaker, D. A., Mukerjee, S., Mitchell, B., Wu, T., Squier, B., Escobar, E., Cousett, T. A., et al. (2016), “South Philadelphia passive sampler and sensor study,” *Journal of the Air & Waste Management Association*, 66, 959–970.
- Tibshirani, R. J. (2014), “Adaptive piecewise polynomial estimation via trend filtering,” *The Annals of Statistics*, 42, 285–323.
- Yuan, M. (2006), “GACV for quantile smoothing splines,” *Computational statistics & data analysis*, 50, 813–829.